

Kinetics of the Superoxide Reductase Catalytic Cycle*[§]

Received for publication, June 18, 2003, and in revised form, August 1, 2003
Published, JBC Papers in Press, August 4, 2003, DOI 10.1074/jbc.M306488200

Joseph P. Emerson, Eric D. Coulter, Robert S. Phillips, and Donald M. Kurtz, Jr.‡

From the Department of Chemistry and Center for Metalloenzyme Studies, University of Georgia, Athens, Georgia 30602

The steady state kinetics of a *Desulfovibrio (D.) vulgaris* superoxide reductase (SOR) turnover cycle, in which superoxide is catalytically reduced to hydrogen peroxide at a [Fe(His)₄(Cys)] active site, are reported. A proximal electron donor, rubredoxin, was used to supply reducing equivalents from NADPH via ferredoxin: NADP⁺ oxidoreductase, and xanthine/xanthine oxidase was used to provide a calibrated flux of superoxide. SOR turnover in this system was well coupled, i.e. ~20₂ reduced:NADPH oxidized over a 10-fold range of superoxide flux. The reduction of the ferric SOR active site by reduced rubredoxin was independently measured to have a second-order rate constant of ~1 × 10⁶ M⁻¹ s⁻¹. Analysis of the kinetics showed that: (i) 1 μM SOR can convert a 10 μM/min superoxide flux to a steady state superoxide concentration of 10⁻¹⁰ M, during which SOR turns over about once every 6 s, (ii) the diffusion-controlled reaction of reduced SOR with superoxide is the slowest process during turnover, and (iii) neither ligation nor deligation of the active site carboxylate of SOR limits the turnover rate. An intracellular SOR concentration on the order of 10 μM is estimated to be the minimum required for lowering superoxide to sublethal levels in aerobically growing SOD knockout mutants of *Escherichia coli*. SORs from *Desulfovibrio gigas* and *Treponema pallidum* showed similar turnover rates when substituted for the *D. vulgaris* SOR, whereas superoxide dismutases showed no SOR activity in our assay. These results provide quantitative support for previous suggestions that, in times of oxidative stress, SORs efficiently divert intracellular reducing equivalents to superoxide.

An emerging paradigm for protecting air-sensitive bacteria and Archaea from the toxic reduction products of dioxygen involves reduction of superoxide and hydrogen peroxide, rather than the classical disproportionation route for their removal characteristic of aerobic microorganisms (1–9). The reduction of superoxide via Reaction 1 is catalyzed by a novel class of non-heme iron enzymes called superoxide reductases (SORs).¹

* The costs of publication of this article were defrayed in part by the payment of page charges. This article must therefore be hereby marked "advertisement" in accordance with 18 U.S.C. Section 1734 solely to indicate this fact.

§ The on-line version of this article (available at <http://www.jbc.org>) contains Table 1S, Figs. S1–S3, and Equations 1S–2.

‡ To whom correspondence should be addressed. Tel.: 706-542-2016; Fax: 706-542-9454; E-mail: kurtz@chem.uga.edu.

¹ The abbreviations used are: SOR, superoxide reductase; SOD, superoxide dismutase; 1Fe-SOR, SOR containing an [Fe(His)₄(Cys)] site as the only prosthetic group; 2Fe-SOR, superoxide reductase containing an accessory [Fe(Cys)₄] site; 2Fe-SOR_{pink}, 2Fe-SOR containing a ferrous [Fe(His)₄(Cys)] site and a ferric [Fe(Cys)₄] site; E47A 2Fe-SOR, recombinant engineered variant of *D. vulgaris* 2Fe-SOR in which the glutamate residue providing the ligand to the ferric [Fe(His)₄(Cys)] site is substituted by an alanine residue; C13S 2Fe-SOR, recombinant



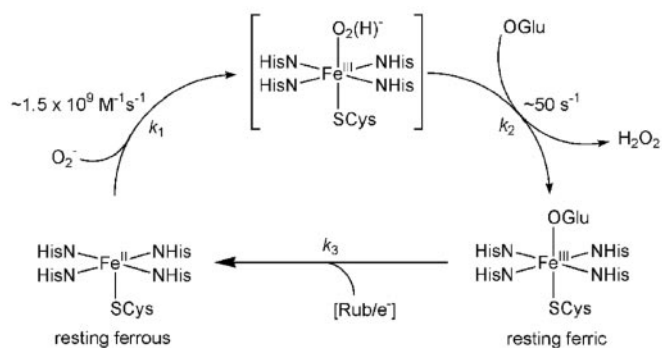
REACTION 1

The SORs are characterized by a mononuclear iron active site shown in Scheme 1 with a ligand set consisting of a square plane of histidine nitrogens, an axial cysteine sulfur and, in the ferric form, a glutamate carboxylate (10, 11).

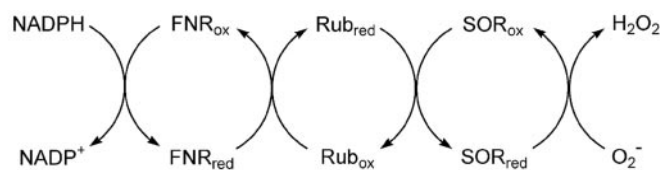
1Fe-SORs contain this site as the only prosthetic group, whereas 2Fe-SORs contain an additional [Fe(Cys)₄] site, the function of which remains enigmatic (12). Kinetics investigations (13, 14) have established that the "resting" ferrous [Fe(His)₄(Cys)] site reacts with superoxide in a diffusion-controlled fashion, producing a transient species, formulated as a ferric-(hydro)peroxo (*cf.* Scheme 1), that at pH ≥ 7 decays in a first-order process to the resting ferric state (14–17). To complete the catalytic cycle the SOR active site must collect an electron for regeneration of the ferrous state. Although superoxide is thermodynamically capable of reducing the ferric SOR site, no such reactivity is apparent, and, as a consequence, SORs show little or no superoxide dismutase (SOD) activity, even when the ligating glutamate carboxylate is replaced by non-coordinating side chains, such as alanine (5, 7, 13, 14).

Neither the kinetics of reduction of the ferric SOR site by other exogenous reducing agents, nor the SOR catalytic turnover cycle have been systematically studied, perhaps because the *in vivo* electron donor(s) to SORs have generally not been established. Thus, no value for the rate constant, *k*₃, in Scheme 1 has been reported for any SOR. The small electron transfer protein, rubredoxin, has been proposed to be a proximal electron donor to both 1Fe- and 2Fe-SORs (5, 18), and, consistent with this suggestion, addition of *Pyrococcus furiosus* 1Fe-SOR resulted in a slight acceleration of rubredoxin oxidation by superoxide (5). In at least two bacteria, the genes for 2Fe-SOR and rubredoxin are co-transcribed (18, 19). For one of these bacteria, the sulfate-reducer, *Desulfovibrio vulgaris*, rubredoxin has been shown to preferentially reduce the [Fe(His)₄(Cys)] site of 2Fe-SOR and to function as the proximal electron donor to 2Fe-SOR in an artificial NADPH:superoxide oxidoreductase reaction cycle shown in Scheme 2 and Equation 2, where FNR is the flavoprotein, spinach ferredoxin:NADP⁺ reductase (20). In this system a calibrated flux of superoxide was generated from reduction of dissolved dioxygen using xanthine and xanthine oxidase, the well established method used to generate superoxide in SOD activity assays (21).

D. vulgaris 2Fe-SOR engineered variant in which the accessory [Fe(Cys)₄] site is absent; C13S 2Fe-SOR_{blue}, C13S 2Fe-SOR containing a ferric [Fe(His)₄(Cys)] site; FNR, spinach ferredoxin:NADP⁺ oxidoreductase; Rub, rubredoxin; *D. vulgaris* H, *Desulfovibrio vulgaris* strain Hildenborough.



SCHEME 1.



SCHEME 2.



REACTION 2

This report describes the kinetics of Reaction 2 using the catalytic system shown in Scheme 2, and analyzes the kinetics according to Scheme 1. The results demonstrate the kinetic competence of both 1Fe- and 2Fe-SORs to lower the steady state superoxide concentration to sublethal levels. The results also quantitate and clarify several qualitative mechanistic observations, presumptions, and speculations in the SOR literature.

EXPERIMENTAL PROCEDURES

Reagents, Proteins, and General Procedures—Reagents and buffers were the highest grade commercially available. All reagents, protein, and media solutions were prepared using water purified with a Millipore ultrapurification system to a resistivity of ~ 18 M Ω to minimize trace metal ion contamination. Bovine milk xanthine oxidase was purchased from Biozyme, Inc. as an ammonium sulfate suspension. Horse heart cytochrome *c*, bovine liver catalase, spinach FNR, *Escherichia coli* Fe-SOD, and bovine Cu/Zn-SOD were purchased from Sigma. Recombinant rubredoxin (20), 2Fe-SOR (15), E47A 2Fe-SOR (13), and C13S 2Fe-SOR (12), all from *D. vulgaris*, and recombinant *Clostridium pasteurianum* rubredoxin (22) was expressed in *E. coli* and purified as described previously. Recombinant *Treponema pallidum* (23) and *Desulfovibrio gigas* 1Fe-SORs (24) were expressed, isolated, and purified by modifications of the published procedures, which are described under Supplemental Materials.

Protein Concentrations and Activities—Concentrations of protein stock solutions were calculated using previously determined molar absorptivities: *D. vulgaris* rubredoxin, $\epsilon_{490} = 8,700$ M $^{-1}$ cm $^{-1}$ (20); *C. pasteurianum* rubredoxin, $\epsilon_{490} = 8,800$ M $^{-1}$ cm $^{-1}$ (25); *D. vulgaris* 2Fe-SOR_{pink} and E47A 2Fe-SOR_{pink}, $\epsilon_{502} = 4,300$ M $^{-1}$ cm $^{-1}$ (13); C13S 2Fe-SOR_{blue}, $\epsilon_{645} = 1,900$ M $^{-1}$ cm $^{-1}$ (12) (with all 2Fe-SOR extinction coefficients per monomer of the homodimer). FNR concentration, catalase, and SOD activities were assumed to be those provided by Sigma.

SOR Activity Assay—The NADPH:superoxide oxidoreductase assay described by Coulter and Kurtz (20) was modified and used as described below. The buffer for all activity measurements and stock solutions was 50 mM phosphate containing 100 μ M EDTA, pH 7.5. All reactions were conducted aerobically at room temperature. In 1 ml of buffer, aliquots of concentrated stock solutions were added to achieve concentrations of 500 μ M xanthine, 1 μ M FNR, ~ 200 units/ml catalase, and 100 μ M NADPH, respectively. The high catalase activity was added to remove hydrogen peroxide, which is not only a product of the SOR reaction but also a by-product of the xanthine/xanthine oxidase superoxide generating system (26). After ~ 30 s rubredoxin was added to a concentration of

1 μ M. Approximately 30 s later either SOR (1 μ M in [Fe(His)₄(Cys)] sites) or SOD (10, 50, 100 or 250 units/ml) were added. After another ~ 30 s, a pre-calibrated amount of xanthine oxidase (typically 5–15 μ l of a stock xanthine oxidase solution prepared by diluting the ammonium sulfate suspension 5-fold with buffer) was added to initiate a flux of superoxide. The superoxide flux generated by the added xanthine oxidase was measured separately both before and after the assay using the same concentrations of xanthine and xanthine oxidase and the same buffer as in the assay mixture and measuring the rate of reduction of horse heart cytochrome *c* ($\epsilon_{550} = 21,500$ M $^{-1}$ cm $^{-1}$), as described previously (20). The rate of NADPH consumption in the SOR assay was measured as the decrease in absorbance at 340 nm ($\epsilon_{340} = 6,220$ M $^{-1}$ cm $^{-1}$). For correlations with superoxide flux, the small background NADPH consumption rate measured prior to addition of xanthine oxidase was subtracted from that measured after the addition of xanthine oxidase. Variations on this protocol are described under “Results.”

Effects of Cyanide and Azide on SOR Activity—The SOR activity assay was conducted as described above, but including small additions of ~ 1 M sodium azide or sodium cyanide stock solutions, to achieve concentrations of either 1 or 20 mM azide or cyanide in the assay mixture. The superoxide flux was pre- and post-calibrated as described above but in the presence of the indicated concentrations of azide or cyanide. For some experiments, *D. vulgaris* 2Fe-SOR or E47A 2Fe-SOR, having concentrations of ~ 860 or ~ 700 μ M in ferrous [Fe(His)₄(Cys)] sites, respectively, were pre-incubated with ~ 20 mM sodium cyanide for ~ 20 h at 4 $^{\circ}$ C. Aliquots of these cyanide-incubated 2Fe-SOR solutions were added to the assay mixture as candidate SORs in the presence of either 1 or 20 mM cyanide in the assay mixture. Further details are given in the text and Table I.

Stopped-flow Monitoring of Reactions of C13S 2Fe-SOR_{blue} with Reduced Rubredoxin—All reactions, column chromatographies, and other manipulations of proteins were conducted in solutions buffered with 50 mM sodium phosphate, pH 7.5, at room temperature, unless otherwise indicated. *D. vulgaris* C13S 2Fe-SOR_{blue} was prepared by aerobically oxidizing ~ 1 ml of as-isolated C13S 2Fe-SOR (~ 500 μ M in [Fe(His)₄(Cys)] sites) by the addition of 2 eq of sodium hexachloroiridate (Aldrich). The oxidized C13S 2Fe-SOR was then passed over a 5-ml Hi-Trap desalting column (Amersham Biosciences). The resulting C13S 2Fe-SOR_{blue} solution was then diluted anaerobically to ~ 400 μ M in [Fe(His)₄(Cys)] sites. Reduced *D. vulgaris* rubredoxin solutions were prepared by purging solutions of ~ 500 μ M oxidized (as-isolated) rubredoxin with argon for 20 min, in a 1-ml quartz cuvette. This sample was then divided into three sealed plastic tubes, and further diluted (~ 5 ml total volume) anaerobically to final concentrations of 80, 40, and 20 μ M rubredoxin. These solutions were again purged with argon for ~ 20 min. These rubredoxin solutions were then reduced by titration with an anaerobic ~ 20 mM sodium dithionite stock solution. The titrations were monitored until addition of a drop (~ 1 μ l) of the sodium dithionite stock solution gave no further decrease in absorbance at 490 nm. The reduced rubredoxin and C13S 2Fe-SOR_{blue} solutions were loaded under an argon purge separately into the two 2.5-ml drive syringes of a RSM-1000 stopped-flow spectrophotometer fitted with a rapid scanning monochromator (OLIS, Inc.). Following stopped-flow mixing, absorbance changes between 350 and 770 nm were monitored by rapid scanning at 25 $^{\circ}$ C.

RESULTS

Specificity of the SOR Activity Assay—Previous work from our laboratory (20) has demonstrated that *D. vulgaris* 2Fe-SOR can serve as the terminal component of the NADPH:superoxide oxidoreductase described by Reaction 2 and Scheme 2. Fig. 1 contains plots of NADPH consumption rates for this SOR assay using various candidate SORs. As shown in Fig. 1, the dimeric *D. vulgaris* 2Fe-SOR, the tetrameric *D. gigas* 1Fe-SOR (a.k.a. neelaredoxin) (27), and the dimeric *T. pallidum* 1Fe-SOR (7, 23), all show very similar activities (listed under Supplemental Materials Table IS). The E47A variant of *D. vulgaris* 2Fe-SOR, in which the ligating glutamate shown in Scheme 1 has been changed to alanine, also shows activity indistinguishable from the wild type protein. Confirming the previous results (20), no NADPH consumption above background occurred upon addition of xanthine oxidase if any of the other protein components were omitted from the assay mixture.

Under the standard SOR assay conditions, but substituting either Cu/Zn- or Fe-SOD at 10, 50, 100, or 250 units/ml (corresponding to low micromolar levels of SOD) in place of SOR,

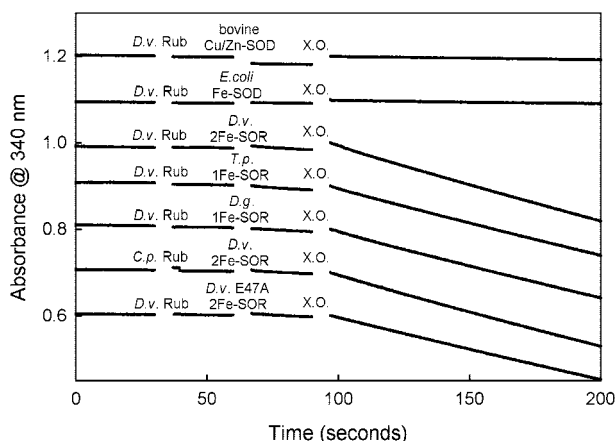


FIG. 1. NADPH:superoxide oxidoreductase activities of *D. vulgaris* (*D.v.*) wild-type and E47A 2Fe-SORs, *T. pallidum* (*T.p.*) 1Fe-SOR, *D. gigas* (*D.g.*) 1Fe-SOR, *E. coli* Fe-SOD, and bovine Cu/Zn-SOD. Rates of NADPH consumption were monitored at room temperature in a 1-ml cuvette as decreases in absorbance at 340 nm in solutions buffered with 50 mM sodium phosphate plus 100 μ M EDTA, pH 7.5, and containing (in the added order): 500 μ M xanthine, 100 μ M NADPH, \sim 200 units/ml catalase, 1 μ M FNR, which constituted the time 0 mixtures. After \sim 30 s, 1 μ M *D. vulgaris* or *C. pasteurianum* (*C.p.*) rubredoxin (*Rub*) was added, and after a further \sim 30 s, either SOR (1 μ M in [Fe(His)₄(Cys)] sites) or SOD (250 units/ml) was added. After obtaining of a baseline NADPH consumption rate, a pre-calibrated amount of xanthine oxidase (*X.O.*) was added at \sim 90 s, producing a superoxide flux of 21.5 ± 2.0 μ M/min. Absorbance spikes caused by the various additions and mixing are omitted from the traces, which are offset vertically by an arbitrary amount for clarity. The NADPH consumption rate for each trace is listed under Supplemental Materials Table 1S.

NADPH was not consumed above background levels. Classical SODs are, thus, not active in this assay at concentrations comparable with SOR, presumably because the SODs cannot accept electrons from any of the donors present in the assay mixture (*i.e.* NADPH, FNR, or rubredoxin) at rates sufficient to outcompete the catalytic disproportionation of superoxide by the SOD. Consistent with this interpretation, the NADPH consumption associated with 2Fe-SOR in the assay was found to be inhibited by Cu/Zn- or Fe-SOD (*cf.* Supplemental Materials Fig. S1). In the case of Cu/Zn-SOD inhibition to background levels could be achieved by \sim 1,000 units/ml. Thus, while classical SODs are not detectably active in the SOR assay, they do compete with SOR for superoxide, as expected (6).

Effects of Cyanide and Azide on SOR Activity—Cyanide and azide are known to bind weakly to both the ferric and ferrous [Fe(His)₄(Cys)] sites of SORs (28–30), and spectroscopic evidence indicates that these anions occupy the coordination site *trans* to the axial cysteine ligand. For this reason, cyanide has been presumed to be an inhibitor of SOR (31), even though no such inhibition data have been published. The data in Table I show that in fact, azide or cyanide at 1 mM caused no substantial inhibition (or activation) of SOR activity using the assay described here. The E47A variant of *D. vulgaris* 2Fe-SOR also was not inhibited by 1 mM cyanide or azide in the assay mixture. In fact, azide or cyanide added to the assay mixture at up to 20 mM showed neither substantial inhibition nor any significant change in the ratio of NADPH consumption rate to SOR flux (*cf.* Table I). However, when *D. vulgaris* 2Fe-SOR (or the E47A variant) was incubated for \sim 20 h with 20 mM cyanide, and this cyanide-preincubated SOR was added to the assay mixture, inhibition was observed, but only if 20 mM cyanide was also present in the assay mixture. The preincubation with a large excess of cyanide results in slow air oxidation of the ferrous [Fe(His)₄(Cys)] site (which is otherwise air-stable) and formation of the ferric [Fe(His)₄(Cys)(CN⁻)] complex (28). Con-

TABLE I
Superoxide flux and NADPH consumption rates in the absence or presence of azide or cyanide in the SOR assay of either wild-type (WT) or E47A *D. vulgaris* 2Fe-SOR

Assays run at room temperature as described under “Experimental Procedures” and the legend to Fig. 1 using 1 μ M *D. vulgaris* 2Fe-SOR (either wild type or E47A) [Fe(His)₄(Cys)] sites in 50 mM sodium phosphate + 100 μ M EDTA, pH 7.6. Ranges are as defined in the legend to Fig. 2.

Inhibitor	Superoxide flux ^a	NADPH consumption rate		CN ⁻ preincubation?
		WT	E47A	
	μ M/min	μ M/min		
None	21.5 ± 2.2	12.4 ± 1.4	11.4 ± 2.5	No
N ₃ ⁻ (1 mM)	24.7 ± 2.9	14.3 ± 1.6	ND ^b	No
CN ⁻ (1 mM)	22.1 ± 2.2	11.9 ± 1.9	12.2 ± 2.5	No
CN ⁻ (20 mM)	21.3 ± 1.5	12.5 ± 1.0	ND	No
CN ⁻ (1 mM)	26.7 ± 1.9	12.0 ± 0.4	11.7 ± 0.6	\sim 20 h/20 mM ^c
CN ⁻ (20 mM)	21.3 ± 1.5	1.7 ± 0.6	ND	\sim 20 h/20 mM ^c

^a Superoxide fluxes were independently calibrated with the same concentrations of azide or cyanide as listed in the Inhibitor column.

^b ND, not determined.

^c 2Fe-SOR was preincubated with 20 mM cyanide at 4 °C for 20 h prior to addition to the SOR assay mixture.

sistent with electrochemical data on synthetic model complexes (31), the binding of cyanide presumably shifts the reduction potential of the ferric [Fe(His)₄(Cys)] site sufficiently negative so that the NADPH/FNR/rubredoxin system is unable to reduce it, thereby blocking electron flow at the SOR_{ox} point of Scheme 2. This pattern of cyanide inhibition provides further confirmation that 2Fe-SOR, and, more specifically, its [Fe(His)₄(Cys)] site, is the terminal catalytic component of the NADPH:superoxide oxidoreductase in this assay.

Stoichiometry and Component Saturation in the SOR Activity Assay—Fig. 2 shows that, when the superoxide flux in the SOR activity assay of *D. vulgaris* 2Fe-SOR was varied over a range of $2.5(\pm 0.4)$ to $37(\pm 1.4)$ μ M superoxide/min, a proportional increase occurred in the NADPH consumption rate. According to Reaction 2, the molar stoichiometry of the NADPH consumption rate to superoxide flux in the steady state should be 1:2. The slope of the fitted line in Fig. 2, \sim 0.56, is consistent with the expected ratio, and shows that under these SOR turnover conditions, essentially all of the superoxide generated by the xanthine/xanthine oxidase system is consumed via the pathway diagrammed in Scheme 2. These results are consistent with those previously reported over a much smaller superoxide flux range (20). Fig. 2 also shows that, under these conditions, the superoxide flux is the rate-limiting process for NADPH consumption.

The concentration of *D. vulgaris* 2Fe-SOR in the activity assay was varied from 50 nM to 10 μ M in [Fe(His)₄(Cys)] sites, while maintaining all other component concentrations and superoxide flux constant at the standard assay levels. A plot of NADPH consumption rate versus 2Fe-SOR concentration under these conditions is shown in Fig. 3. Approximately 0.5 μ M 2Fe-SOR is needed to reach maximum consumption of NADPH under the standard conditions. A least-squares fit of the Michaelis-Menten equation to the data gave the solid curve shown in Fig. 3 with V_{\max} of 11.6 ± 0.3 μ M NADPH consumed per min and apparent $K_{m(\text{app})}$ of \sim 100 nM 2Fe-SOR (at a superoxide flux of 21.3 ± 0.7 μ M/min). The physical meaning of this $K_{m(\text{app})}$ is ambiguous. However, because from Fig. 2, the rate-limiting step at saturating 2Fe-SOR is production of superoxide, then, at less-than-saturating 2Fe-SOR concentrations (<0.5 μ M from Fig. 2), the rate-limiting step must become the reaction of 2Fe-SOR with either superoxide or reduced rubredoxin.

An analogous set of experiments was conducted in which the concentration of *D. vulgaris* rubredoxin was varied between 50

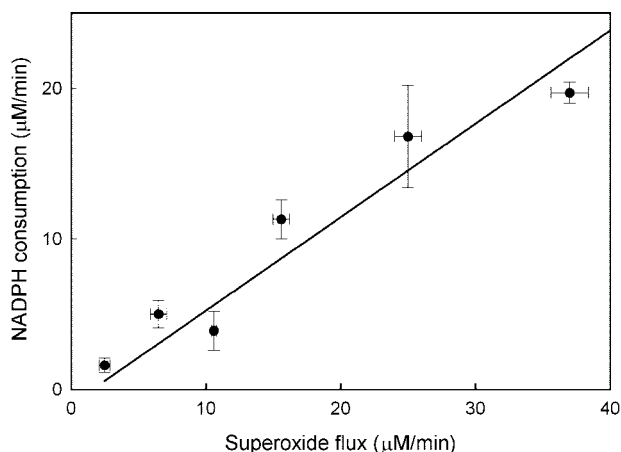


FIG. 2. **Superoxide flux dependence on NADPH consumption in the SOR activity assay.** NADPH consumption rates were monitored as shown in Fig. 1 and under the conditions described in the legend to Fig. 1 using $1 \mu\text{M}$ *D. vulgaris* rubredoxin and $1 \mu\text{M}$ *D. vulgaris* 2Fe-SOR [Fe(His)₄Cys] sites. Plotted NADPH consumption rates were corrected for background consumption prior to addition of xanthine oxidase. Superoxide fluxes were independently measured both before and after the assays, and the error bars indicate the standard deviations of the averages of at least five measurements of superoxide fluxes and three determinations of NADPH consumption rates.

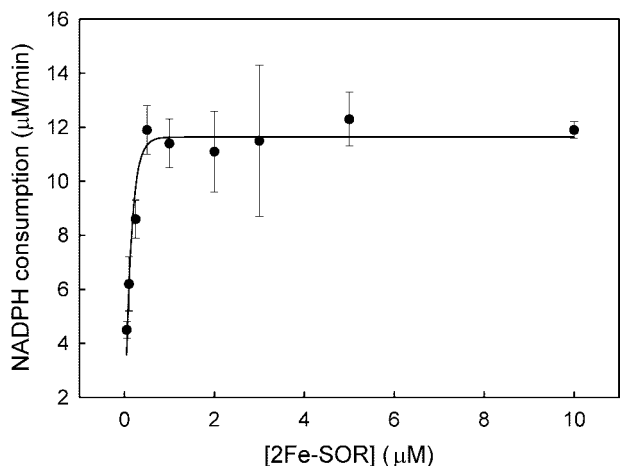


FIG. 3. **Dependence of NADPH consumption rate on *D. vulgaris* 2Fe-SOR concentration in the SOR activity assay.** Rates of NADPH consumption were monitored as described and shown in Fig. 1 with $1 \mu\text{M}$ *D. vulgaris* Rub, 50 nM to $10 \mu\text{M}$ 2Fe-SOR [Fe(His)₄Cys] sites, and a pre-calibrated amount of xanthine oxidase to produce a superoxide flux of $21.3 (\pm 0.7) \mu\text{M}/\text{min}$. Plotted NADPH consumption rates are corrected for the small background consumption prior to addition of xanthine oxidase. Error bars represent the standard deviation of three or more measurements at each 2Fe-SOR concentration.

nM and $10 \mu\text{M}$ while maintaining all other concentrations and superoxide flux constant at the standard levels. A plot of the NADPH consumption rates versus concentration of rubredoxin is shown in Fig. 4. Approximately $0.45 \mu\text{M}$ rubredoxin was needed for the maximum NADPH consumption rate under these conditions. A fit of the Michaelis-Menten equation to the data gave V_{max} of $11.8 \pm 0.2 \mu\text{M}/\text{min}$, and $K_{\text{m(app)}}$ of $\sim 100 \text{ nM}$ rubredoxin (at a superoxide flux of $19.9 \pm 0.8 \mu\text{M}/\text{min}$). Thus, at $<0.45 \mu\text{M}$ rubredoxin, the rate-limiting step must become either the reduction of rubredoxin by FNR or reduction of 2Fe-SOR by rubredoxin. Varying the concentrations of FNR ($0.25\text{--}2 \mu\text{M}$) or NADPH ($50\text{--}300 \mu\text{M}$) had very little effect on the superoxide-dependent NADPH consumption rates measured in this assay (*cf.* Supplemental Materials Figs. S2 and S3). The 2Fe-SOR/rubredoxin reaction (corresponding to the step with rate constant k_3 in Scheme 1) must, therefore,

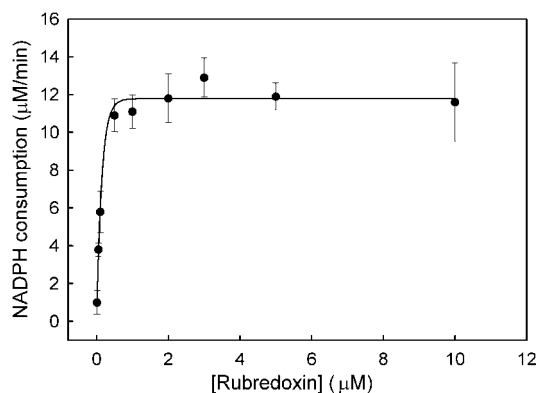


FIG. 4. **Dependence of NADPH consumption rate on *D. vulgaris* rubredoxin concentration in the SOR activity assay.** Rates of NADPH consumption were monitored as described and shown in Fig. 1 using 50 nM to $10 \mu\text{M}$ *D. vulgaris* rubredoxin, $1 \mu\text{M}$ *D. vulgaris* 2Fe-SOR [Fe(His)₄Cys] sites, and a pre-calibrated amount of xanthine oxidase to produce a superoxide flux of $19.9 (\pm 0.8) \mu\text{M}/\text{min}$. Plotted NADPH consumption rates are corrected for the small background consumption prior to addition of xanthine oxidase. Error bars represent the standard deviations of three or more measurements at each rubredoxin concentration.

become rate-limiting only at submicromolar concentrations of rubredoxin under our assay conditions.

Kinetics of SOR Reduction by Rubredoxin—The rate constant for *D. vulgaris* 2Fe-SOR reduction by *D. vulgaris* rubredoxin was measured by stopped-flow mixing of excess reduced rubredoxin with C13S 2Fe-SOR_{blue}. This 2Fe-SOR variant contains the ferric [Fe³⁺(NHis)₄(SCys)] site but lacks the [Fe(SCys)₄] site, the ferric absorption of which is very similar to that of rubredoxin and, therefore, interferes with spectrophotometric monitoring of the rubredoxin oxidation (12). Fig. 5 shows that the reaction progress was monitored as the increase in absorbance at 490 nm ($\epsilon_{490} 8,700 \text{ M}^{-1} \text{ cm}^{-1}$) associated with the ferric [Fe(SCys)₄] site of oxidized rubredoxin, as well as the decrease in absorbance at 650 nm associated with the ferric [Fe(His)₄(Cys)] site of C13S 2Fe-SOR_{blue}. The reactions were conducted under approximately pseudo-first order conditions with excess C13S 2Fe-SOR_{blue} ($\epsilon_{650} 1,900 \text{ M}^{-1} \text{ cm}^{-1}$). Under the conditions used for these experiments, the earliest obtainable spectra ($\sim 1 \text{ ms}$ after mixing) indicated that nearly 75% of the rubredoxin in solution had oxidized within the mixing dead time. The changes in absorption ended $\sim 10 \text{ ms}$ after mixing. Because of the rapid time scale of this reaction, only the last $\sim 25\%$ of the reaction could be measured, which resulted in relatively large uncertainties in the kinetics fits, especially for the relatively small decreases in absorbance at 650 nm . Therefore, only the 490-nm data are reported in Table II. The average k_{obs} of $\sim 240 \text{ s}^{-1}$ coupled with the C13S 2Fe-SOR_{blue} concentration of $200 \mu\text{M}$ used in these experiments leads to an estimated second-order rate constant of $1.2 \times 10^6 \text{ M}^{-1} \text{ s}^{-1}$ for the reduced rubredoxin/C13S 2Fe-SOR_{blue} electron transfer reaction. The fact that this value is about 4 times greater than the previously reported electron self-exchange rate constant for rubredoxin, $\sim 3 \times 10^5 \text{ M}^{-1} \text{ s}^{-1}$, can be qualitatively rationalized by the $\sim 300 \text{ mV}$ driving force for the reduced rubredoxin/oxidized 2Fe-SOR electron transfer reaction (12, 32) and the protein-surface accessible, solvent-exposed [Fe(His)₄(Cys)] site of 2Fe-SOR (10). The limited amounts of C13S 2Fe-SOR available and the rapidity of the reaction prevented a more thorough kinetic analysis. Because we have previously shown that C13S 2Fe-SOR reacts with superoxide in a manner indistinguishable from that of the wild type protein (12), the second-order rate constant listed above can be taken as an estimate of k_3 in Scheme 1 for the wild type 2Fe-SOR.

FIG. 5. Rapid-scanning stopped-flow spectroscopy of the absorbance changes following mixing of C13S 2Fe-SOR_{blue} with reduced rubredoxin at 25 °C in 50 mM sodium phosphate, pH 7.5. An anaerobic solution of reduced rubredoxin was stopped-flow mixed (1:1) (v/v) with a C13S 2Fe-SOR_{blue} solution, resulting in concentrations of 20 μM rubredoxin ferrous [Fe(Cys)₄] sites and 200 μM C13S 2Fe-SOR_{blue} ferric [Fe(His)₄(Cys)] sites immediately after mixing. The first spectrum (with the lowest A₄₉₀ nm and highest A₆₅₀ nm) was obtained ~1 ms after mixing, and subsequent spectra at 2-ms intervals until 10 ms. *Inset* shows corresponding absorbance versus time traces at 490 and 650 nm.

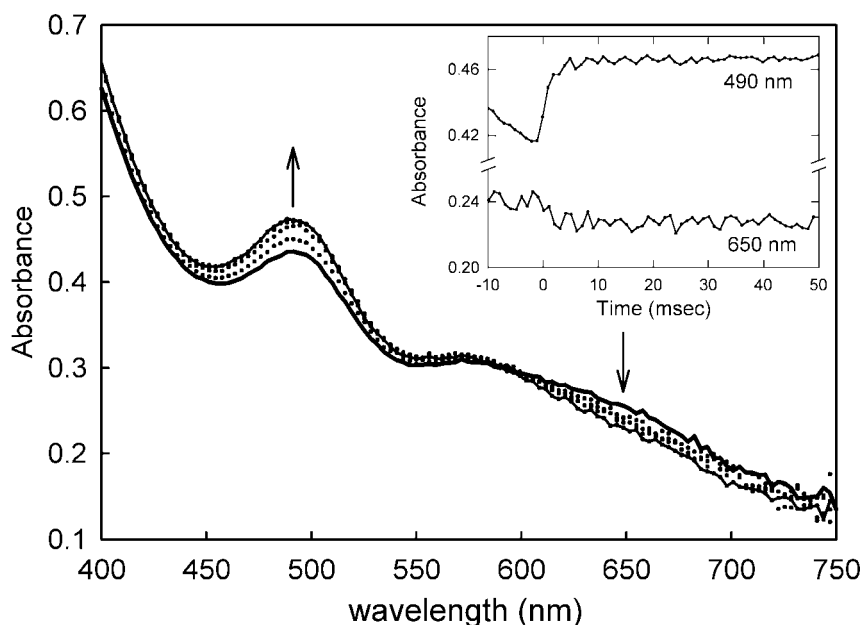


TABLE II

Observed rate constants for stopped-flow reactions of reduced *D. vulgaris* rubredoxin with excess *D. vulgaris* C13S 2Fe-SOR_{blue}

[Rubredoxin]	k_{obs}^a s ⁻¹
μM	
40	360 ± 40
20	255 ± 100
10	100 ± 70

^a Rate constants are based on the assumption that all of the rubredoxin was in the ferrous state when the reaction was initiated.

DISCUSSION

Detection of SOR Activity—In our hands the assay described here consistently performs as a means of measuring SOR activity of both 1Fe- and 2Fe-SORs. The SOR specificity and low detection limit (<50 nM SOR) suggests that this assay could be used to detect SORs in cellular extracts and/or during isolation and purification, particularly in organisms that do not contain SODs (which compete with SOR for superoxide). Fig. 1 shows that *C. pasteurianum* rubredoxin, which is commercially available, as are all the other assay components, can be substituted for the *D. vulgaris* rubredoxin in the SOR assay.

Analysis of SOR Turnover Kinetics—Together with our previous results (12, 13, 15), we now have experimental measurements for all three rate constants, k_1 , k_2 , and k_3 in Scheme 1 for *D. vulgaris* 2Fe-SOR. The results presented in the text, Table I, and Figs. 2–4 demonstrate that, under the standard SOR assay conditions, NADPH consumption and superoxide generation are tightly coupled and that the superoxide flux limits the turnover rate. Under the steady state conditions of the SOR assay, we can then make the following assumptions: (i) all steps in Scheme 1 are irreversible; (ii) the measured superoxide flux, ν_{SOR} , is equivalent to the rate of superoxide consumption via Schemes 1 and 2; (iii) rubredoxin is essentially all in its reduced form, *i.e.* the reduced rubredoxin concentration equals the total rubredoxin concentration, [Rub_T]; and (iv) the total SOR concentration, [SOR_T], is the sum of the concentrations of resting ferrous ([SOR_{red}]), intermediate ([SOR_{int}]), and resting ferric ([SOR_{ox}]) species in Scheme 1,

$$[\text{SOR}_T] = [\text{SOR}_{\text{red}}] + [\text{SOR}_{\text{int}}] + [\text{SOR}_{\text{ox}}] \quad (\text{Eq. 1})$$

Using the Flux Method (33), which assumes equal flux (= ν_{SOR}) through all steps in the steady state, Equation 2 is then readily derived (*cf.* Supplemental Materials) from Equation 1.

$$[\text{SOR}_T]/\nu_{\text{SOR}} = 1/k_1[\text{O}_2^-] + 1/k_2 + 1/k_3[\text{Rub}_T] \quad (\text{Eq. 2})$$

Equation 2 expresses simply that the total turnover time, [SOR_T]/ ν_{SOR} , is the sum of the transit times for each step in Scheme 1.

Numerical comparisons of the various terms in Equation 2 provide several mechanistic insights regarding Scheme 1. First, knowing only the superoxide flux (~10 μM/min ≡ 0.17 μM/s under our standard assay conditions) and [SOR_T] (1 μM), we can estimate the total turnover time, [SOR_T]/ ν_{SOR} , to be ~6 s. That is, a given SOR molecule reacts with superoxide approximately once every 6 s under our assay conditions. This turnover time is consistent with a very low steady state superoxide concentration. Rearranging Equation 2 to Equation 3,

$$[\text{O}_2^-] = \frac{1/k_1}{[\text{SOR}_T]/\nu_{\text{SOR}} - 1/k_2 - 1/k_3[\text{Rub}_T]} \quad (\text{Eq. 3})$$

and using the values of k_1 and k_2 listed in Scheme 1 (13, 15), the value of k_3 determined in this work, and the values of ν_{SOR} , [Rub_T], and [SOR_T] used in our standard SOR assay (0.17 μM/s, 1 and 1 μM, respectively), the calculated steady state [O₂⁻] = 1.3 × 10⁻¹⁰ M. At such low concentrations, spontaneous disproportionation of superoxide, occurring with second-order rate constant ~5 × 10⁵ M⁻¹ s⁻¹ at pH 7.5 (34), is extremely slow compared with our assay time scales, and, could, therefore, not compete with the steady state reaction cycle in Scheme 1. Second, the decay of the intermediate (1/ k_2 ~0.02 s), and reduction of the ferric [Fe(His)₄(Cys)] site, (1/ k_3 [Rub_T] ~0.8 s) both occur much more rapidly than the diffusion-controlled encounter of superoxide with the ferrous [Fe(His)₄(Cys)] site (1/ k_1 [O₂⁻] ~5 s), *i.e.* the total turnover time is dominated by the first term on the right side of Equation 2. Thus, most (~86%) of the SOR is in its reduced form (SOR_{red}) during steady state turnover under the conditions described here. Finally, the decay of the intermediate to the resting ferric state, (1/ k_2 ~0.02 s), occurs much faster than reduction (1/ k_3 [Rub_T] ~0.8 s). The incoming glutamate carboxylate shown in Scheme 1, therefore, has ample time to ligate the ferric SOR site prior to its re-reduction. Removal of this ligating glutamate does not appreciably affect turnover time; the E47A 2Fe-SOR (in which this glutamate is changed to an alanine) showed activity that was indistinguishable from the wild type in the SOR assay (*cf.* Fig. 1 and Table I). We and others have previously shown that k_2 is

unaffected by the E47A substitution at and above neutral pH (13, 17). Fig. 3 shows that a >2-fold decrease from the standard 1 μM concentration of rubredoxin leads to detectably lower NADPH consumption rates, which, based on Equation 2, means that a factor of >2 increase in the $1/k_3[\text{Rub}_T]$ term is sufficient to detectably slow down turnover. The lack of effect of the E47A substitution, therefore, implies that this substitution does not lead to an appreciable (>2-fold) decrease in k_3 . Thus, neither ligation nor deligation of this carboxylate is rate-limiting for SOR turnover under the assay conditions. The E47A 2Fe-SOR variant was also able to complement SOD knockout strains of *E. coli* (17)² (see discussion below), indicating that this variant is functional *in vivo*. The E47A substitution does not confer substantial SOD activity on 2Fe-SOR (13). The “purpose” of this conserved glutamate ligand, thus, remains mysterious. Ligation by this glutamate may inhibit side reactions, such as with H_2O_2 . The E47A variant appears to be somewhat more reactive than wild type with excess H_2O_2 (13, 35).

In Vivo Relevance—Whereas no estimates of superoxide levels are available for anaerobic microorganisms exposed to air, the steady state superoxide concentration of $\sim 10^{-10}$ M calculated for our SOR assay is the same as the steady state cytoplasmic superoxide concentration estimated for aerobically growing *E. coli* (36), and this level was analyzed to be barely sublethal (37). Expression of either 2Fe- or 1Fe-SORs, including the *D. vulgaris* 2Fe-SOR examined here, has been shown to restore aerobic growth to SOD knockout mutants of *E. coli* (which contains no SOR homolog) (1, 7, 8, 24) and to lower intracellular superoxide levels in such strains (4). This lowering presumably occurs via pathways analogous to those of Schemes 1 or 2, but must use a proximal electron donor other than rubredoxin (which is not present in *E. coli*). The superoxide flux estimated for aerobic, exponentially growing *E. coli* is about an order of magnitude higher than could be achieved using the xanthine/xanthine oxidase system in our SOR activity assay (36, 37). To analyze the turnover of SOR under such conditions we can simplify Equation 3 as follows. Under our assay conditions with $\sim 10^{-10}$ M steady state $[\text{O}_2^-]$, $[\text{SOR}_T]/\nu_{\text{SOR}} \gg 1/k_2$ as discussed above, and the term equivalent to $1/k_3[\text{Rub}_T]$ must also be small compared with $[\text{SOR}_T]/\nu_{\text{SOR}}$, because the SOR appears to be fully reduced prior to breaking the SOD knockout *E. coli* cells expressing the SORs (6)^{2,3}. Therefore, under the growth conditions of the SOR-complemented *E. coli* strains, Equation 3 can be approximated by Equation 4.

$$[\text{O}_2^-] \cong \frac{1/k_1}{[\text{SOR}_T]/\nu_{\text{SOR}}} = \frac{\nu_{\text{SOR}}}{k_1[\text{SOR}_T]} \quad (\text{Eq. 4})$$

According to Equation 4, an order of magnitude higher superoxide flux would require an order of magnitude higher $[\text{SOR}_T]$ to maintain approximately the same steady state $[\text{O}_2^-]$. We can, thus, estimate that the intracellular $[\text{SOR}_T]$ concentration in complemented SOD knockout *E. coli* strains must be on the order of at least 10 μM (in active sites) to maintain $[\text{O}_2^-]$ at $\leq 10^{-10}$ M. This lower limit of intracellular SOR concentration is about the same as the estimated SOD concentration in wild type *E. coli* (36–38). Presuming that intracellular superoxide must be reduced to approximately the same low level for survival of anaerobic microorganisms exposed to air, and,

because 10^{-10} M is less than one molecule per bacterial cell, this analysis emphasizes that, like SODs, SORs function in large excess over their steady state substrate concentration, as is the case in our SOR activity assay.

Thus, on the basis of the ability to lower superoxide concentrations, SORs and SODs appear to be about equally efficient at scavenging superoxide. SODs, however, do not require a source of reducing equivalents, which might seem to constitute an advantage over SORs for scavenging of superoxide. However, in the glucose-grown, aerobically respiring SOD knockout *E. coli* strains, sufficient reducing equivalents are provided to recombinantly expressed SOR such that its turnover lowers superoxide to non-lethal levels (1, 7, 8, 24). In aerobic bacteria the flux of reducing equivalents through the membrane-bound respiratory chain is considered to be the main generator of cytoplasmic superoxide via adventitious one-electron reduction of dioxygen (38, 41, 42). As has been pointed out (38), because only a minute fraction ($\sim 0.1\%$) of the total respiratory reducing flux is diverted to produce superoxide, the reducing equivalents that would need to be diverted to reduce this superoxide via SOR must also be a minute fraction of those passing through the respiratory chain. It has, in fact, been proposed that, under the relatively reducing conditions of the bacterial cytoplasm, SODs might also function as SORs (38, 43). We have not, however, detected SOR activity for either Cu/Zn- or Fe-SODs using our assay.

Many “strictly” anaerobic sulfate-reducing bacteria have the ability to reduce dioxygen (44), and a functional cytochrome *bd*-type membrane-bound terminal oxidase has been isolated from *D. gigas* (45). The *D. vulgaris* strain Hildenborough (H) is the source of the rubredoxin and 2Fe-SOR examined in this work. The *D. vulgaris* H genome contains genes encoding both cytochrome *c*- and *bd*-type membrane-bound terminal oxidases (46). The function of these “respiratory” oxidases is unclear, because these sulfate-reducing bacteria do not grow aerobically. One possible function is dioxygen scavenging upon exposure to air, which would thereby generate a superoxide flux. *D. vulgaris* H, which remains viable after up to a few hours incubation in air-saturated media (8, 46), contains a periplasmic SOD and a single cytoplasmic SOR, the 2Fe-SOR examined in this work (8). A mutant *D. vulgaris* H strain in which the SOR is inactivated was clearly more sensitive than the wild type to both air exposure and to paraquat-induced increases in cytoplasmic superoxide fluxes (8, 46). A limiting factor in aerobic survival of *D. vulgaris* H may be the *in vivo* lifetime of 2Fe-SOR. This protein gradually disappeared from air-exposed *D. vulgaris* H cells (46), presumably because of damaging reactions in the increasingly oxidizing environment. In its natural growth habitat *D. vulgaris* may more often be exposed to subaerobic levels of dioxygen (44, 47, 48), which may be lowered even further by reduction in the periplasm (46, 49). The cytoplasmic superoxide flux under such conditions is unknown but is unlikely to be significantly higher than that of dioxygen-respiring aerobic bacteria.

The activities in the SOR assay of the 1Fe-SORs from *D. gigas* and *T. pallidum* (the latter of which is a microaerophile and contains no classical SOD), are indistinguishable from that of *D. vulgaris* 2Fe-SOR. The *D. gigas* and *T. pallidum* 1Fe-SORs were also able to complement SOD knockout *E. coli* strains (7, 24), once again relying on non-native electron donors. The relatively long turnover times, coupled with the high reduction potentials of SOR active sites (>200 mV versus NHE) (12), helps explain how non-native donor(s) in *E. coli* can furnish reducing equivalents for viable intracellular SOR turnover and suggests that SORs may use more than one proximal electron donor even in the native organism. The values of k_1 for

² J. P. Emerson and D. M. Kurtz, Jr., unpublished results.

³ In the case of the 2Fe-SORs, this conclusion is based on the lack of a red color in whole cells or freshly prepared cell extracts that would arise from the more strongly absorbing ferric $[\text{Fe}(\text{Cys})_4]$ site. This site must, therefore be fully (or nearly so) reduced. Note that the ferric $[\text{Fe}(\text{Cys})_4]$ site in 2Fe-SORs has a lower reduction potential and is harder to reduce than the ferric $[\text{Fe}(\text{His})_4(\text{Cys})]$ site (cf. Ref. 20). The color due to the ferric $[\text{Fe}(\text{Cys})_4]$ site of 2Fe-SOR gradually develops upon exposure of the cell extracts to air.

four different 1Fe- and 2Fe-SORs are all on the order of $10^9 \text{ M}^{-1} \text{ s}^{-1}$, whereas the values of k_2 equal or exceed those listed in Scheme 1 (7, 13, 14, 50). Presuming similarly high values of k_3 to that measured for *D. vulgaris* 2Fe-SOR (and/or higher concentrations of proximal electron donor(s) than used in our assay), Equation 4 implies that, in the presence of an adequate supply of reducing equivalents, all of the characterized SORs should lower steady state superoxide levels with about equal efficiency, which is limited by the diffusion-controlled reaction of the ferrous SOR active site with superoxide (the k_1 term in Equation 4). The results reported here, thus, provide quantitative support for previous suggestions (3, 20) that, in times of intracellular oxidative stress, SORs function as relatively promiscuous electron acceptors but specific electron donors to superoxide, *i.e.* under such conditions SORs efficiently funnel intracellular reducing equivalents to superoxide.

Acknowledgments—We thank Amy C. Luce for experimental assistance and Radu Silaghi-Dumitrescu for helpful discussions.

REFERENCES

- Pianzola, M. J., Soubes, M., and Touati, D. (1996) *J. Bacteriol.* **178**, 6736–6742
- Kurtz, D. M., Jr., and Coulter, E. D. (2001) *Chemtracts. Inorg. Chem.* **14**, 407–435
- Kurtz, D. M., Jr., and Coulter, E. D. (2002) *J. Biol. Inorg. Chem.* **7**, 653–658
- Liochev, S. I., and Fridovich, I. (1997) *J. Biol. Chem.* **272**, 25573–25575
- Jenney, F. E., Jr., Verhagen, M. F. J. M., Cui, X., and Adams, M. W. W. (1999) *Science* **286**, 306–309
- Lombard, M., Fontecave, M., Touati, D., and Niviere, V. (2000) *J. Biol. Chem.* **275**, 115–121
- Lombard, M., Touati, D., Fontecave, M., and Niviere, V. (2000) *J. Biol. Chem.* **275**, 27021–27026
- Lumppio, H. L., Shenvi, N. V., Summers, A. O., Voordouw, G., and Kurtz, D. M., Jr. (2001) *J. Bacteriol.* **183**, 101–108
- Abreu, I. A., Xavier, A. V., LeGall, J., Cabelli, D. E., and Teixeira, M. (2002) *J. Biol. Inorg. Chem.* **7**, 668–674
- Coehlo, A. V., Matias, P., Fülöp, V., Thomson, A., Gonzalez, A., and Carrondo, M. A. (1997) *J. Biol. Inorg. Chem.* **2**, 680–689
- Yeh, A. P., Hu, Y., Jenney, F. E., Jr., Adams, M. W., and Rees, D. C. (2000) *Biochemistry* **39**, 2499–2508
- Emerson, J. P., Cabelli, D. E., and Kurtz, D. M., Jr. (2003) *Proc. Natl. Acad. Sci. U. S. A.* **100**, 3802–3807
- Emerson, J. P., Coulter, E. D., Cabelli, D. E., Phillips, R. S., and Kurtz, D. M., Jr. (2002) *Biochemistry* **41**, 4348–4357
- Abreu, I. A., Saraiva, L. M., Soares, C. M., Teixeira, M., and Cabelli, D. E. (2001) *J. Biol. Chem.* **276**, 38995–39001
- Coulter, E. D., Emerson, J. P., Kurtz, D. M., Jr., and Cabelli, D. E. (2000) *J. Am. Chem. Soc.* **122**, 11555–11556
- Silaghi-Dumitrescu, R., Silaghi-Dumitrescu, I., Coulter, E. D., and Kurtz, D. M., Jr. (2003) *Inorg. Chem.* **42**, 446–456
- Lombard, M., Houee-Levin, C., Touati, D., Fontecave, M., and Niviere, V. (2001) *Biochemistry* **40**, 5032–5040
- Brumlik, M. J., and Voordouw, G. (1989) *J. Bacteriol.* **171**, 4996–5004
- Das, A., Coulter, E. D., Kurtz, D. M., and Ljungdahl, L. G. (2001) *J. Bacteriol.* **183**, 1560–1567
- Coulter, E. D., and Kurtz, D. M., Jr. (2001) *Arch. Biochem. Biophys.* **394**, 76–86
- McCord, J. M., and Fridovich, I. (1969) *J. Biol. Chem.* **244**, 6049–6055
- Richie, K. A., Teng, Q., Elkin, C. J., and Kurtz, D. M., Jr. (1996) *Protein Sci.* **5**, 883–894
- Jovanovic, T., Ascenso, C., Hazlett, K. R., Sikkink, R., Krebs, C., Litwiller, R., Benson, L. M., Moura, I., Moura, J. J., Radolf, J. D., Huynh, B. H., Naylor, S., and Rusnak, F. (2000) *J. Biol. Chem.* **275**, 28439–28448
- Silva, G., LeGall, J., Xavier, A. V., Teixeira, M., and Rodrigues-Pousada, C. (2001) *J. Bacteriol.* **183**, 4413–4420
- Lovenberg, W., and Walker, M. N. (1978) *Methods Enzymol.* **53**, 340–346
- Fridovich, I. (1970) *J. Biol. Chem.* **245**, 4053–4057
- Chen, L., Sharma, P., Le Gall, J., Mariano, A. M., Teixeira, M., and Xavier, A. (1994) *Eur. J. Biochem.* **226**, 613–618
- Romao, C. V., Liu, M. Y., Le Gall, J., Gomes, C. M., Braga, V., Pacheco, I., Xavier, A. V., and Teixeira, M. (1999) *Eur. J. Biochem.* **261**, 438–443
- Silva, G., Oliveira, S., Gomes, C. M., Pacheco, I., Liu, M. Y., Xavier, A. V., Teixeira, M., Legall, J., and Rodrigues-Pousada, C. (1999) *Eur. J. Biochem.* **259**, 235–243
- Clay, M. D., Jenney, F. E., Jr., Hagedoorn, P. L., George, G. N., Adams, M. W. W., and Johnson, M. K. (2002) *J. Am. Chem. Soc.* **124**, 788–805
- Shearer, J., Fitch, S. B., Kaminsky, W., Benedict, J., Scarrow, R. C., and Kovaacs, J. A. (2003) *Proc. Natl. Acad. Sci. U. S. A.* **100**, 3671–3676
- Eidsness, M. K., Burden, A. E., Richie, K. A., Kurtz, D. M., Jr., Scott, R. A., Smith, E. T., Ichiye, T., Beard, B., Min, T., and Kang, C. (1999) *Biochemistry* **38**, 14803–14809
- Waley, S. G. (1992) *Biochem. J.* **286**, 357–359
- Bielski, B. H. J., Cabelli, D. E., and Arudi, R. L. (1985) *J. Phys. Chem. Ref. Data* **14**, 1041–1100
- Mathe, C., Mattioli, T. A., Horner, O., Lombard, M., Latour, J.-M., Fontecave, M., and Niviere, V. (2002) *J. Am. Chem. Soc.* **124**, 4966–4967
- Imlay, J. A., and Fridovich, I. (1991) *J. Biol. Chem.* **266**, 6957–6965
- Gort, A. S., and Imlay, J. A. (1998) *J. Bacteriol.* **180**, 1402–1410
- Imlay, J. A. (2002) *J. Biol. Inorg. Chem.* **7**, 659–663
- Deleted in proof
- Deleted in proof
- Messner, K. R., and Imlay, J. A. (2002) *J. Biol. Chem.* **277**, 42563–42571
- Imlay, J. A. (1995) *J. Biol. Chem.* **270**, 19767–19777
- Liochev, S. I., and Fridovich, I. (2000) *J. Biol. Chem.* **275**, 38482–38485
- Cypionka, H. (2000) *Annu. Rev. Microbiol.* **54**, 827–848
- Lemos, R. S., Gomes, C. M., Santana, M., LeGall, J., Xavier, A. V., and Teixeira, M. (2001) *FEBS Lett.* **496**, 40–43
- Fournier, M., Zhang, Y., Wildschut, J. D., Dolla, A., Voordouw, J. K., Schriemer, D. C., and Voordouw, G. (2003) *J. Bacteriol.* **185**, 71–79
- Eschemann, A., Kéuhl, M., and Cypionka, H. (1999) *Environ. Microbiol.* **1**, 489–494
- Johnson, M. S., Zhulin, I. B., Gapuzan, M. E., and Taylor, B. L. (1997) *J. Bacteriol.* **179**, 5598–5601
- Baumgarten, A., Redenius, I., Kranczoch, J., and Cypionka, H. (2001) *Arch. Microbiol.* **176**, 306–309
- Niviere, V., Lombard, M., Fontecave, M., and Houee-Levin, C. (2001) *FEBS Lett.* **497**, 171–173